Published in final edited form as:
Neuroscience. 2011 January 26; 173: 57–75. doi:10.1016/j.neuroscience.2010.11.006.

Importance of genetic background for risk of relapse shown in altered prefrontal cortex gene expression during abstinence following chronic alcohol intoxication

Joel G. Hashimoto, MS[1,2], **Melissa R. Forquer, BA**[1], **Michelle A. Tanchuck, BS**[2], **Deborah A. Finn, PhD**[1,2], and **Kristine M. Wiren, PhD**[*,1,2,3]

[1]Research Service, Portland Veterans Affairs Medical Center, Oregon Health & Science University, Portland, Oregon 97239

[2]Department of Behavioral Neuroscience, Oregon Health & Science University, Portland, Oregon 97239

[3]Department of Medicine, Oregon Health & Science University, Portland, Oregon 97239

Abstract

Alcoholism is a relapsing disorder associated with excessive consumption after periods of abstinence. Neuroadaptations in brain structure, plasticity and gene expression occur with chronic intoxication but are poorly characterized. Here we report identification of pathways altered during abstinence in prefrontal cortex, a brain region associated with cognitive dysfunction and damage in alcoholics. To determine the influence of genetic differences, an animal model was employed with widely divergent responses to alcohol withdrawal, the Withdrawal Seizure-Resistant (WSR) and Withdrawal Seizure-Prone (WSP) lines. Mice were chronically exposed to highly intoxicating concentrations of ethanol and withdrawn, then left abstinent for 21 days. Transcriptional profiling by microarray analyses identified a total of 562 genes as significantly altered during abstinence. Hierarchical cluster analysis revealed that the transcriptional response correlated with genotype/withdrawal phenotype rather than sex. Gene Ontology category overrepresentation analysis identified thyroid hormone metabolism, glutathione metabolism, axon guidance and DNA damage response as targeted classes of genes in low response WSR mice, with acetylation and histone deacetylase complex as highly dimorphic between WSR and WSP mice. Confirmation studies in WSR mice revealed both increased neurotoxicity by histopathologic examination and elevated T3 levels. Most importantly, relapse drinking was reduced by inhibition of thyroid hormone synthesis in dependent WSR mice compared to controls. These findings provide *in vivo* physiological and behavioral validation of the pathways identified. Combined, these results indicate a fundamentally distinct neuroadaptive response during abstinence in mice genetically selected for divergent withdrawal severity. Identification of pathways altered in abstinence may aid development of novel therapeutics for targeted treatment of relapse in abstinent alcoholics.

Keywords

alcoholism; chronic ethanol; abstinence; relapse; microarray; gene expression

[*]*Address correspondence to*: Kristine Wiren, PhD, OHSU and VA Medical Center, Research Service P3R&D-39, (telephone number: 503.220.8262.56595), (fax number: 503.273.5351), (wirenk@ohsu.edu) .

Alcohol (ethanol; EtOH) abuse and dependence, a chronic relapsing disease, is a well recognized public health problem and one of the most common disorders in the western world. In general, the alcohol addiction cycle has been described as consisting of three stages: intoxication, withdrawal and craving/abstinence (Koob and Volkow, 2010). One characteristic of alcoholism is uncontrolled excessive consumption of alcohol, characterized by an inability to remain abstinent. Abstinence from alcohol drinking is an important goal for the treatment of alcoholism, but there is limited understanding of factors that influence risk of relapse and as a result, few effective treatments (Olive, 2010).

As the central nervous system is a primary target of alcohol, it has been proposed that changes in brain architecture, plasticity and/or function that result from chronic abuse can increase liability for relapse during a period of abstinence (Valdez and Koob, 2004). Thus, despite weeks, months, or years of sobriety, the brain of an alcoholic remains different from a non-alcoholic. As an example, brain damage associated with alcohol abuse in selected brain regions is well documented, but the extent of recovery during abstinence remains controversial (Gazdzinski et al., 2005, Pfefferbaum et al., 2006). Long-lived adaptations that result from chronic alcohol abuse are thought to be manifested at least in part by changes in steady-state gene expression. Identification of targets that remain altered in abstinence after chronic EtOH exposure is critical for development of a better understanding of relapse liability (Wiren et al., 2006). However, there is little data available identifying such neuroadaptive changes during abstinence, and there have been no transcriptional profiling analyses undertaken to date to characterize expression differences in the brain observed after a defined period of abstinence following chronic EtOH intoxication.

Evidence of physical dependence is considered another hallmark of alcoholism. One measure of physical dependence is increased neuronal excitability, including seizures, associated with withdrawal from EtOH. Hyperexcitability during withdrawal is thought to reflect neuroadapations that occur with chronic EtOH intoxication that enable an organism to function in the presence of this CNS depressant and thus re-establish internal homeostasis. Estimates suggest that over 25% of heavy drinking alcoholics can suffer from seizures (Wetterling et al., 1999). In addition, there is substantial heritability (40 – 60% in twin studies) in the susceptibility to EtOH addiction (Magnusson et al., 2010), consistent with genetic risk factors. Given that alcoholism is a disorder of complex genetics that is influenced by interactions between the environment and multiple susceptible genetic loci, dissecting genetic contributions to the disease is difficult. Thus, various animal models have been developed that show increased or decreased sensitivity to EtOH. The use of selected lines provides a genetically rich model where the various alleles present in the initial heterogeneous population related to the selection phenotype become differentially segregated in the respective mouse lines. Here we employed lines of mice with highly divergent withdrawal severity after chronic intoxication derived by selective breeding; the lower responding Withdrawal Seizure-Resistant (WSR) and higher responding Withdrawal Seizure-Prone (WSP) mouse lines (Kosobud and Crabbe, 1986). These lines are of interest because they show large differences in neuroadaptation to chronic alcohol, as evidenced by divergent withdrawal severity.

In addition, sex differences are observed in many EtOH-related behaviors, including liability for and the development of EtOH dependence, EtOH sensitivity and consumption, and differences in withdrawal severity (Brady and Randall, 1999, Devaud and Chadda, 2001, Sershen et al., 2002, Wang et al., 2003a, Carroll et al., 2004, Prescott et al., 2005). Female rodents tend to consume more alcohol yet have reduced withdrawal severity, including in the WSP and WSR selected lines (Kosobud and Crabbe, 1986). Gender differences have also been reported in terms of alcohol handling (Addolorato et al., 1999), and females have reduced levels of alcohol dehydrogenase, a key liver enzyme involved in alcohol

metabolism and removal (Baraona et al., 2001). Given the importance of both genetic background and gender (biological sex), we have examined both sexes employing WSR and WSP selected lines to evaluate the influence of genetic factors vs. sex on the neuroadaptive response observed during abstinence following chronic EtOH exposure. We previously demonstrated a sex-specific response to chronic alcohol during peak withdrawal in prefrontal cortex (PFC) transcription profiles in these two selected lines, with the result that both WSP and WSR females showed increased vulnerability to brain damage while only modest differences were observed between the lines (Hashimoto and Wiren, 2008). In the present study, expression profiling was performed at 21 d of abstinence. Differences in PFC gene expression were identified, as PFC is damaged by alcohol abuse (Matsumoto, 2009) and is a central brain region in cognition, mediating executive function and inhibitory control (Leh et al., 2010). Expression differences were identified using microarray hybridization, with bioinformatic analysis by unsupervised hierarchical and *k*-means cluster analysis. Differences in expression were confirmed by quantitative reverse-transcription polymerase chain reaction (qRT-PCR) analysis. Biological functions of genes significantly regulated were characterized with Gene Ontology (GO), with interacting pathways identified. Changes in biological outcomes derived from pathway analysis were evaluated to validate the expression differences identified. Through expression profiling of PFC isolated during a period of abstinence following chronic intoxication and withdrawal, we sought to identify underlying biological targets for treatment to reduce relapse drinking in abstinent populations.

Experimental Procedures

Animal Subjects

Two independently-derived replicate WSP and WSR lines (Kosobud and Crabbe, 1986) were derived by selective breeding for divergent withdrawal severity from genetically heterogeneous HS/Ibg mice. Female and male mice from both replicates (*i.e.*, WSP-1, WSP-2 and WSR-1, WSR-2), obtained from Dr. Crabbe (Portland, OR), were tested for expression differences. To identify phenotype-specific differences, expression analysis was collapsed on replicate for each selected line. Confirmation of biological pathways was performed in replicate-1 mice. Mice were maintained under a light/dark cycle of 0600-1800 light with water and Purina Lab Diet chow available *ad libitum*. Room temperatures were maintained at 22 ± 1° C. All animal procedures were approved by the Portland Oregon VA Medical Center Institutional Animal Care and Use Committee and followed US National Institutes of Health animal welfare guidelines.

Abstinence Following Chronic EtOH Intoxication and Brain Harvest

Mice were made dependent upon EtOH by the Alcohol Dependence Core of the Portland Alcohol Research Center, using a method of vapor inhalation in chambers manufactured in-house, with modifications previously published (Beadles-Bohling and Wiren, 2006). Drug-naïve adult mice from selected generation 26 (filial generations G87 - G116) were used. EtOH exposure was initiated at 0800 h. On day one EtOH mice were weighed, injected intraperitoneally (i.p.) with EtOH at 1.5 g/kg for WSP-1, WSR-1 and WSR-2 and 1.75 g/kg for WSP-2 animals, and 68.1 mg/kg pyrazole HCl (Pyr; an alcohol dehydrogenase inhibitor used to maintain constant blood EtOH levels). This is a standard procedure to ensure that similar blood EtOH concentrations (BECs) are maintained between the selected lines (Terdal and Crabbe, 1994). Control animals were placed into air chambers and received Pyr only. Although Pyr has been shown to interact with NMDA receptors as both an agonist and antagonist, depending on concentration (Pereira et al., 1992), a saline-only air control was not included because previous data had shown that there was no observable difference between saline and Pyr treated animals with respect to broad profiles of gene expression

analyzed at the lower level of sensitivity of mRNA differential display (Wiren unpublished observations and Schafer et al., 1998). All mice again received Pyr (68.1 mg/kg) at 24 h and 48 h to reduce fluctuations in BEC. Since Pyr is an alcohol dehydrogenase inhibitor that prevents the metabolism of alcohol, its use can limit production of alcohol metabolites during the exposure period. However, since Pyr has a 10 h half-life in mice (Goldstein and Pal, 1971) and the final dose was given 24 h prior to removal from the chambers, the inhibitory effects on EtOH metabolism would be greatly diminished during the withdrawal period and abstinence phase. EtOH exposed mice had 20 μl of blood taken from the tail for daily BEC determination. Following 72 h of constant EtOH vapor exposure, all mice were removed from the chambers, weighed, and had tail blood samples drawn for BEC determination by gas chromatography as previously described (Beadles-Bohling and Wiren, 2006). All animals used in these experiments were purposely not scored for handling-induced convulsions (HICs) to limit the effects of withdrawal seizures *per se* on measurements of both gene expression and brain damage. During withdrawal these mice typically show decreased activity, dysphoria, and mild tremor in some animals. However, without handling, the mice do not exhibit convulsions. Brain tissue was harvested for RNA analysis from animals after 21 d abstinence. PFC was isolated by dissection from whole brain by first discarding the olfactory bulb and making a coronal slice 2 mm into the frontal region of the cortex. Lateral regions were removed by cutting the tissue at a 45° angle with the lobes facing upward. Tissues were snap frozen in liquid nitrogen and stored at −80°C until processing.

Animals used for brain histology were deeply anesthetized with mouse cocktail (ketamine 7.5 mg/ml, xylazine 0.75 mg/ml, acepromazine 0.15 mg/ml; 0.01 ml/g mouse body weight) and perfused transcardially with cold 0.9% saline followed by 4% paraformaldehyde in 0.1M phosphate buffered saline (PBS). Brains were then isolated and fixed in 4% paraformaldehyde in 0.1M PBS overnight.

Chemicals

EtOH (ethyl alcohol, absolute, 200 proof) for use in chemical assays was purchased from AAPER Alcohol and Chemical (Shelbyville, KY), and Pharmco Products, Inc. (Brookfield, CT) for use in the EtOH vapor chambers and injections. Pyr was purchased from Sigma-Aldrich Chemical Co. (St. Louis, MO) and dissolved in 0.9% saline (NaCl). EtOH (20% v/v) was mixed with 0.9% saline and injected i.p. or introduced without mixing as a vapor into the chambers. Methimazole (MMI) and sucrose were from Sigma-Aldrich. In the EtOH drinking study, mice consumed a sweetened EtOH solution (5% w/v sucrose + 10% v/v EtOH in tap water).

RNA Isolation and GeneFilter Microarray Processing

Total RNA was isolated and treated as previously described (Hashimoto and Wiren, 2008). Probe labeling from the total RNA mixture was performed by linear synthesis with ^{33}P-dATP incorporation using the Array Advantage kit (Ambion, Austin, TX). Five micrograms of total RNA from two mice were pooled for each hybridization for a total of 32 microarray hybridizations (4 arrays (2 arrays per replicate line), 2 sexes, 2 lines, 2 treatments). Microarray hybridization with complex labeled RNA probe was performed overnight at 50° C with 20 ml Ultraarray Hybridization Buffer (Ambion, Austin, TX). The final post-hybridization wash was at 50°C in 0.5X SSC, 0.5% SDS similar to standard Northern blot procedures. Research Genetics GF400 mouse microarrays (Invitrogen, Carlsbad, CA) employed for these studies contained 4300 unique mouse cDNA accessions (both genes and ESTs) that average 1500 bp in length, generally with one spot per cDNA. Background hybridization values (typically very low) were subtracted from each hybridization value. One array was excluded from analysis based on determination of correlation coefficients

values below 90% for 'replicate' arrays and was replaced with a separate hybridization from RNA from the same treatment, sex, line. Several advantages are notable with the use of cDNA arrays. First, the gene sets chosen were highly enriched in expressed sequences with known functions, improving our ability to characterize the biological consequences of expression differences. Furthermore, the longer hybridization sequences allow for higher stringency in the hybridization and wash procedures for greater gene specificity (Dai et al., 2005). One limitation of the low density array is that a number of EtOH modulated genes will be missed because of lack of representation on the platform we employed. Generation of the complex probe is performed by linear reverse transcription, *i.e.*, without additional steps or amplification procedures that potentially skew probe populations. Thus, the higher sensitivity of cDNA arrays using radioactive detection (Bertucci et al., 1999) is particularly advantageous in the identification of differences in EtOH regulated transcription, known to show only modest regulation (Treadwell et al., 2004, Hashimoto and Wiren, 2008).

Microarray Data Analysis

Microarrays were exposed to storage phosphor screens for two hours and scanned at high resolution with a Cyclone phosphorimager (Packard Bell-Perkin Elmer, Shelton, CT). Data from all samples were $\log_2$ transformed, converted to z-scores, multiplied by 2 and added to 8 so that each array had a mean of 8, a variance of 4, and a standard deviation of 2 (WebQTL, Wang et al., 2003b). This conversion procedure results in a 1 unit expression difference corresponding to a 2-fold change in expression. The level of expression of each gene or expressed sequence tag (EST) was determined using OptiQuant software and imported into Pathways v4 software (Research Genetics, Carlsbad, CA). Raw expression values were then exported, normalized, and analyzed using Vector Xpression 3.1 (Invitrogen, Carlsbad, CA). Expression differences were determined using an uncorrected Student's *t*-test (n = 4 for each group, two-tailed, $\alpha = 0.05$) to identify a large group of differentially regulated transcripts (Rodd et al., 2007). For this approach, it was important to identify a large number of EtOH regulated genes which then could be mined for significant enrichment in biological processes or functions using GO, followed by confirmation analysis. Expression differences in a subset of genes were confirmed by qPCR as previously described (Hashimoto and Wiren, 2008). Briefly, qRT-PCR was performed with the iCycler IQ Real Time PCR detection system (Bio-Rad Laboratories, Inc., Hercules, CA) using a one-step QuantiTect SYBR Green RT-PCR kit (Qiagen, Valencia, CA) on DNase-treated total RNA (Hashimoto et al., 2004). Relative expression of the RT-PCR product was determined using the comparative $\Delta\Delta C_t$ method, after normalizing expression to total RNA measured with RiboGreen (Molecular Probes, Eugene, OR, USA) (Hashimoto et al., 2004). Primers were purchased pre-designed from Qiagen (Valencia, CA)

All significantly regulated transcripts were used in an unsupervised hierarchical cluster analysis (average linkage, Euclidian distance) with 100 resampling iterations to determine Bootstrap values for each node using the TIGR Multiple Experiment Viewer (TMEV) software from The Institute For Genomic Research (Saeed et al., 2003). Additional analysis using *k*-means clustering was carried out using TMEV with the number of clusters set to 32, average linkage, and Euclidian distance metric.

To identify cellular pathways and biological themes that were affected during EtOH withdrawal, we used DAVID (the Database for Annotation, Visualization and Integrated Discovery v6.7; http://david.niaid.nih.gov/david/ease.htm) and Gene Ontology Tree Machine (GOTM) to assign genes to the categories of the Gene Ontology Consortium (www.geneontology.org) and to test statistically for significant coregulation (Dennis et al., 2003, Zhang et al., 2004, Huang da et al., 2009). Functional association networks were constructed to identify hypothetical interactions or relationships between regulated genes that might not have formal GO annotations using Pathway Architect, part of the

GeneSpringGX 10.0 suite (Agilent Technologies, Santa Clara, CA, USA). The data presented in this analysis are available at NCBI's Gene Expression Omnibus (GSE23165).

Assessment of EtOH induced brain damage

Saggital blocks of each brain were processed by dehydration, paraffin infiltration, and embedding as previously described (Hashimoto and Wiren, 2008). Adjacent 6 μm saggital sections were made. Three contiguous images were captured (904 μm × 675 μm each) that encompassed the PFC (Lateral 0.36 – 0.72; Bregma 2.8-3.5; Interaural 2.5-5.3) of the right hemisphere using an AxioPlan2e microscope (Carl Zeiss MicroImaging, Inc, Thornwood, NY) at 100X magnification. Full thickness of each image was analyzed by counting dead cells using MetaMorph software v6.2 (Universal Imaging Corporation, Downingtown, PA, USA). Dead or dying cells were identified in hemotoxylin and eosin (H&E) stained sections (Hashimoto and Wiren, 2008). All counts were conducted with the investigator blind to treatment, selected line, and sex.

Assessment of thyroid hormone metabolism by serum T3 analysis

Blood was collected by terminal cardiac puncture under anesthesia at 21 d of abstinence. Serum was harvested and stored at −80°C until analysis. Total triiodothyronine (T3) levels were determined by enzyme linked immunoassay following the manufacturer's recommendations (MP Biomedical Santa Ana, CA). The detection limit was 0.24 ng/ml, with an 8.3% intra-assay coefficient of variation.

Behavioral analysis with relapse drinking

To develop an animal model of EtOH relapse drinking, WSR and WSP male mice were first trained to drink an EtOH solution, using a modified sucrose fading procedure. Mice were individually housed with 24 h access to fluids that were presented in two inverted 25 ml glass graduated cylinders with metal sippers, and a modified sucrose fading procedure was used to slowly introduce EtOH to a 5% w/v sucrose (5S) solution constituted in tap water. Increasing concentrations of EtOH were added to the 5S solution, ending with 1 month of access to 5S+10% EtOH (10E). Measurement of drinking followed standard laboratory procedures (Yoneyama et al., 2008), and the EtOH dose consumed was calculated from the average volume depleted after correcting for body weight. At the end of the training procedure, there were no line differences in consumption of the sweetened EtOH solution between WSR and WSP males [1.93 ± 0.30 g/kg (n = 15) versus 2.27 ± 0.51 g/kg (n = 16) respectively].

To produce withdrawal-induced relapse drinking, a modification of the intermittent vapor exposure procedure (Becker and Lopez, 2004, Griffin et al., 2009a, Griffin et al., 2009b) with periods of abstinence to produce an alcohol deprivation effect (ADE, Melendez et al., 2006), was used. Increased EtOH intake following repeated bouts of intermittent exposure with ADE has been described as a model of relapse drinking (Becker and Lopez, 2004, Sanchis-Segura and Spanagel, 2006, Morrow et al., 2009). Thus, several bouts of chronic intoxication in conjunction with periods of abstinence would model relapse drinking associated with a history of dependence. Briefly, mice were exposed to chronic intoxication using the 72 h vapor procedure on three separate occasions, separated by periods of voluntary consumption of sweetened EtOH (5S+10E) or water (abstinence) in a 24 h access two-bottle choice procedure (see Figure 5A for timeline of tests). Following the 3rd exposure to 72 h of EtOH vapor, WSR males previously exposed to EtOH intoxication and withdrawal demonstrated increased voluntary relapse drinking versus controls, while EtOH intake in WSP mice was not different. WSR males were thus chosen to examine candidate pathways that might reduce relapse drinking. Modulation of thyroid hormone signaling was achieved using the small molecular inhibitor MMI. After the measurement of EtOH intake

for 3 d, both groups of WSR mice (e.g., control and repeated 72 h EtOH vapor) were injected with MMI (i.p., 60 mg/kg/d; daily for 5d) to inhibit thyroid hormone production and induce hypothyroidism (Cano-Europa et al., 2010). The effect on voluntary EtOH consumption was evaluated daily.

Statistical analyses

Data were analyzed using Prism v5.03 software (GraphPad Software, Inc., San Diego, CA), SYSTAT 11 (SYSTAT Software Inc., Point Richmond, CA), and Vector Xpression 3.1 (Invitrogen, Carlsbad, CA). Differences of $p < 0.05$ were considered statistically significant. Results are presented as the mean ± SEM. Individual differences in gene expression were analyzed by two-tailed *t*-test between EtOH treated and control samples from each sex and line. Differences in EtOH relapse drinking were evaluated by two-tailed *t*-test between control or repeatedly EtOH withdrawn male WSR mice. BECs during EtOH exposure were analyzed by two-way ANOVA (sex x selected line), using Bonferonni's test in post-hoc analysis.

Results

Chronic EtOH exposure and synchronized withdrawal

We have characterized the neuroadaptive gene expression differences after 21 d abstinence, from chronic EtOH exposure followed by synchronized withdrawal. We chose 21 d of abstinence based on a variety of reports documenting physiological and behavioral differences that remained for weeks after withdrawal (Valdez et al., 2003, Brooks et al., 2008, Nixon et al., 2008, Williams et al., 2009, Hansson et al., 2010). At the onset of the experiments, animals were 69.4 d ± 0.6 (range 44 - 82 d), and body weights were 24.7 g ± 0.2 (range 17.8 - 32.3 g). During exposure, blood EtOH concentrations (BECs) were monitored daily and EtOH vapor levels were modified to achieve a highly intoxicating level with BECs of 2.1 - 2.4 mg/ml (46 - 52 mM). Importantly, these blood levels are above the legal limit (17 mM or 0.08% is the legal limit for driving in most US states) and are within the range seen (2.0-3.0 mg/ml) in most alcoholic patients (Adachi et al., 1991). Average BECs over the 72 h exposure ranged from 1.6 - 3.2 mg/ml (34 - 70 mM) with an overall average BEC of 2.3 mg/ml (50 mM). The average BEC for each group were as follows: male WSP 2.8 ± 0.2 mg/ml (60 mM), male WSR 2.0 ± 0.1 mg/ml (43 mM), female WSP 2.4 ± 0.2 mg/ml (51 mM), and female WSR 2.2 ± 0.1 mg/ml (48 mM). Two-way ANOVA showed no differences in BEC between selected line, sex, or interaction of selected line by sex.

EtOH regulated transcripts during abstinence following chronic intoxication

In this study, we modeled the abstinence stage at 21 d after withdrawal from chronic EtOH intoxication, one of the three stages (intoxication, withdrawal and craving/abstinence) of the addiction cycle (Koob and Volkow, 2010). Gene expression differences that result from acute and chronic EtOH intoxication are pervasive but fold differences are modest (Treadwell et al., 2004, Hashimoto and Wiren, 2008). Given this, identification of significant differences is dependent on a methodological approach with high sensitivity but low background. The array analysis employed here has several advantages for reliable detection of modest expression differences that include synchronized withdrawal after high intoxication (that is difficult to achieve in human populations) and an array platform that utilizes radioactive detection, longer probe length for stable hybridization and nylon membranes with low background following stringent washes. Using this approach, we identified 562 genes that were regulated during abstinence following chronic EtOH intoxication and a 21 d extended withdrawal period. Expression differences were modest, with most ratios less than 1.3. We used an uncorrected *p*-value, as we have done previously

(Hashimoto and Wiren, 2008), to decrease the chance of excluding transcripts regulated during abstinence (*i.e.*, false negatives). qPCR was used to confirm gene regulation identified by microarray hybridization analysis. Genes were selected for confirmation based on function and represented genes that covered the range of regulation as identified by microarray hybridization analysis. A comparison is shown between the level of expression difference identified by qPCR vs. that identified in the array analysis in Table 1 with confirmation of 28 out of 32 genes, or ~88%. This rate of confirmation is consistent with our previous array analysis that used a similar approach to detect modest expression differences (Hashimoto and Wiren, 2008), and the confirmation rate is high relative to other array platforms and analytical approaches (see Treadwell et al., 2004, see Tang et al., 2006).

Differential gene expression in WSR and WSP during abstinence

Among the 562 genes identified, the numbers of regulated genes were similar between groups. Female WSP had 111 genes regulated during abstinence, 164 genes were regulated in Male WSP, 154 genes were regulated in female WSR, and 218 genes were regulated in male WSR mice. Overall, the number of sequences identified during abstinence is slightly higher than that identified at peak withdrawal after chronic intoxication (Hashimoto and Wiren, 2008). A comparison between genes regulated at peak withdrawal vs. genes regulated during abstinence revealed 108 genes as significant in both analyses. Of these EtOH-regulated genes, the majority showed the same direction of response between the two time-points, with 38 % regulated similarly in the same group while only 7 % were regulated in the opposite direction (i.e., up- vs. down-regulation in the same group). Finally, comparisons of naïve animals between selected lines (WSP vs. WSR) found 480 differentially expressed genes (sexes collapsed). Of the 562 genes regulated during abstinence, 157 (28 %) were differentially expressed between naïve WSP and WSR.

One factor that may be important in evaluating the impact of gene expression differences identified during abstinence is the extent or level of regulation observed for specific transcripts. Table 2 lists the most highly up- or down-regulated sequences in male and female WSR and WSP mice. As noted, the expression differences detected in general were modest, with no ratios higher than ±1.3.

Bioinformatic analysis of pathways regulated during abstinence following chronic intoxication

Unsupervised hierarchical cluster analysis was performed to determine the similarity of global expression profiles in significantly regulated genes (Figure 1a). Each column represents combined data from eight arrays for one experimental analysis [4 control vs. 4 EtOH, for each sex (F, M) and genotype/withdrawal phenotype (R, P)] to visualize the transcriptional response in abstinence after chronic intoxication in each individual condition. Genes are depicted based on the expression ratio for the effect of EtOH vs. control with shades of color to indicate EtOH withdrawal up-regulation (red), down-regulation (green) or no difference (black) for a given gene in all conditions. The top dendrogram displays similarity of gene expression for the four experimental groups; relatedness of the arrays is denoted by distance to the node linking the arrays. The two most dissimilar experimental clusters in overall differential gene expression in abstinence following chronic intoxication and withdrawal were split primarily upon the genotype/withdrawal phenotype and not the sex of the mice (*i.e.*, female and male WSP were grouped together as related, as were male and female WSR). Thus, clustering analysis identified genotype/withdrawal phenotype, not sex, as contributing the strongest influence on expression patterns. Bootstrap analysis confirmed the importance of genotype/withdrawal phenotype, where black nodes indicates 100% support of the tree topology for separation based on genotype, green nodes indicate 70 - 80% support and yellow nodes indicate 60 - 70% support for similarity of the two sexes for

each genotype (Figure 1a). Thus, the microarray experiments during abstinence after chronic intoxication grouped together based on genetic background, not sex, as we previously observed at the peak withdrawal time-point in WSP and WSR mice (Hashimoto and Wiren, 2008).

To identify specific groups of genes that demonstrated highly divergent expression patterns between WSP and WSR mice, *k*-means clustering of was used. A total of 32 clusters were identified, with 11 of the clusters identifying genes with a highly dimorphic response between WSP and WSR, as shown in Figure 1b and 1c. Highly dimorphic clusters in Figure 1 (b and c) are color-coded (left of each cluster) and shown in the hierarchical cluster analysis to the right of Figure 1a. Not surprisingly, gene clusters from k-means analysis tended to group together in hierarchical cluster analysis.

Gene pathway enrichment analysis

To identify biological signaling pathways that were influenced by abstinence in each selected line and sex, computational characterization with gene ontology (GO) enrichment analysis was used to group significantly regulated genes into similar biological or molecular functional categories. For this analysis, we employed DAVID using the list of genes significantly differentially regulated. We first characterized GO groups statistically overrepresented in the regulated sequences that were identified in cluster analysis shown in Figure 1b and 1c as the most dimorphic between WSR and WSP mice (Table 3). For GO enrichment analysis of highly dimorphic genes between WSP and WSR, we used a *p*-value cut off of 0.1 to increase the number of identified categories, as the number of genes used in this analysis was relatively small (i.e., 36 down-regulated genes for WSR, 60 up-regulated genes for WSR). Notably, this analysis identified ‘AT hook DNA binding’, ‘acetylation’ and ‘histone deacetylase complex’ groups as overrepresented in the highly dimorphic expression differences. We next employed DAVID and GOTM analysis to identify GO groups statistically overrepresented in the class of regulated sequences for each group characterized (i.e., female WSR, male WSR, female WSP, and male WSP) using the list of genes significantly differentially regulated from each 21 d comparison (Table 4). For GO enrichment analysis for each group of EtOH regulated genes, we used a *p*-value cut off of 0.05. GO enrichment analysis identified the biological process ‘thyroid hormone metabolism’ as an overrepresented in male WSP and female WSR groups. Of note, the genes (*Ttr*, *Dio2*) that were regulated in the ‘thyroid hormone metabolism’ category were up-regulated in WSR females but down-regulated in WSP males. ‘Glutathione metabolism’ and ‘axon guidance’ was significantly overrepresented in WSR males. ‘DNA damage response, signal transduction’ was significantly modulated in WSR females. The category ‘spliceosome complex’ was overrepresented in WSP male and female mice, while ‘lipid metabolism’ and ‘lipid biosynthesis’ were significant categories in male WSR and WSP, respectively.

To identify functional relationships between regulated genes that may not have formal GO annotations, network association analysis was performed. Using the ‘Biological Process’ relevance network in Pathway Architect, we identified ‘apoptosis’ as a central node in male WSR, male WSP, and female WSP networks. Interestingly, in the male WSR network, most of the genes connected with the apoptosis node were up-regulated while in both male and female WSP mice, the genes associated with apoptosis were down-regulated by abstinence from EtOH (Figure 2). Hierarchical cluster analysis of the genes associated with apoptosis showed clear separation of the microarray experiments based on selected line versus sex, suggesting a differential response based on line at 21 d abstinence following chronic intoxication. In other words, WSR male and female mice had increased apoptotic signaling and more up-regulated transcripts, but WSP male and female mice had less apoptotic signaling.

Physiological and behavioral validation of identified pathways

Based on the bioinformatic analysis suggesting that the PFC of WSR mice had increased apoptosis/cell death related signaling 21 d following chronic EtOH intoxication, we analyzed the PFC for increased dead or dying cells in WSR and WSP mice (Figure 3A). For the evaluation of neurodegeneration, saggital sections were stained with H&E. Dead cells were clearly identified as cells with an angular pyknotic nucleus and a hypereosinophilic cytoplasm (Figure 3C; note cell morphology in zoomed images as insets). Counting of dead cells was performed as described in *Experimental Procedures*. Cell counts in the PFC comparing control and abstinent mice at 21 d showed a significant increase in dead cells in WSR males ($p < 0.05$) and a trend in females, but no difference in WSP male or female mice (Figure 3B). This result is consistent with the expression differences identified and the results of the bioinformatic analyses.

In order to identify potential small molecules that could be utilized in therapeutic settings, additional bioinformatic analysis using the 'Small Molecule' network in Pathway Architect was performed. We focused on networks that were dimorphic between the selected lines, based on the importance of genotype in the overall transcriptional response in abstinence. Using this approach, 'TTR' (transthyretin) was identified as a central node in both WSR and WSP networks, which was enhanced in WSR mice but reduced in WSP mice (Figure 4A). TTR is an important serum carrier for thyroxine (Thx) and retinol, and among other functions is a mediator of thyroid hormone action (Richardson, 2007). Given that alcohol exposure and withdrawal have been shown to influence thyroid hormone levels (Valimaki et al., 1984, Baumgartner et al., 1994, Pienaar et al., 1995, Ozsoy et al., 2006) and to further confirm the relevance of the expression differences identified, we measured total serum T3 levels at 21 d after chronic EtOH intoxication in WSR and WSP male and female mice. T3 levels were determined by enzyme linked immunoassay following the manufacturer's recommendations (MP Biomedical Santa Ana, CA). As shown in Figure 4B, T3 levels in WSR male and female mice were significantly elevated but there were no changes in WSP males or females (Figure 4B), again consistent with network analysis.

Finally, we evaluated the potential influence of modulation of the regulated pathways on relapse drinking as behavioral validation of the significant expression differences between abstinent WSR and WSP mice. Males were chosen because both sexes were similar in pathway analysis. A model of withdrawal-induced relapse drinking was used with three rounds of chronic exposure and withdrawal (timeline in Figure 5A), in which half the mice were exposed to control conditions and half to chronic EtOH intoxication and withdrawal using vapor inhalation as described in Experimental Procedures. BECs did not differ upon removal from the vapor chambers at the end of the procedure between WSP and WSR mice following the 1st round [1.84 ± 0.15 mg/ml (n = 11) and 1.80 ± 0.11 mg/ml (n = 12), respectively] and 2nd round [0.33 ± 0.19 mg/ml (n = 10) and 0.01 ± 0.01 mg/ml (n = 10), respectively] of vapor exposures, but were higher in the WSP [1.28 ± 0.11 mg/ml (n = 8)] vs. WSR [0.76 ± 0.15 mg/ml (n = 7)] mice following the 3rd round. Following each round of chronic exposure and withdrawal, mice were monitored for voluntary alcohol consumption (Test) in a two-bottle choice 24 h access paradigm for at least one week (10 - 17 d), with intervening periods of abstinence of generally 3 d intervals before and after drinking. This procedure produced increased voluntary relapse drinking in WSR mice but not in WSP mice, as shown in Figure 5B. Significant increases in voluntary EtOH drinking were observed after the first and third cycle of chronic intoxication and withdrawal in the WSR line, to 155 % (Test 1) and 169 % (Test 3) over controls, respectively. The lack of effect on drinking after the 2nd cycle of vapor exposure was likely due to the very low EtOH exposure that was achieved in those animals, since recent work suggested that a sustained BEC of 1.75 mg/ml during chronic EtOH exposure was important for the subsequent escalation in EtOH drinking (Griffin et al., 2009a). Thus, using this paradigm, WSR mice demonstrated

relapse drinking but WSP mice did not. Having established increased drinking in the WSR mice, we then evaluated whether interference of a pathway that had been identified as significantly different during abstinence would reduce voluntary relapse drinking. Thyroid hormone signaling was chosen as a candidate pathway on the basis of several findings: we observed enhanced thyroid hormone related signaling in network analysis, 'thyroid gland development' and 'hormone stimulus' as GO overrepresented categories, and confirmation of significantly increased T3 levels in WSR mice during abstinence (see Figure 4a,b). Methimazole (MMI) is an antithryoid drug that inhibits thyroid hormone signaling *in vivo* through inhibition of thyroperoxidase activity to block the addition of iodine to thyroglobulin, a necessary step in the synthesis of thyroid hormones including T3 and T4. Increased relapse drinking was observed daily for 3 d (as shown in Figure 5c), then on the third day after voluntary consumption access, WSR control and previously intoxicated mice were administered MMI (60 mg/kg/d) each morning for 5 consecutive days (d 3 – d 7) and alcohol preference was again monitored by two-bottle choice (Figure 5c). Inhibition of thyroid hormone signaling significantly reduced voluntary EtOH relapse drinking in male WSR mice that were previously exposed to chronic EtOH intoxication compared to control animals ($p < 0.05$ on d 7 and 8 of the procedure). MMI administration was stopped on d 7 of the procedure. Previously intoxicated WSR mice demonstrated a subsequent reversal of the inhibition of increased relapse drinking by d 10.

Discussion

The aim of this study was to characterize the neuroadaptive changes in WSR and WSP male and female mice using microarray and expression profiling bioinformatic analyses during abstinence from chronic EtOH. Our results identified significant expression differences in the mouse PFC after a period of abstinence from chronic EtOH intoxication, which was strongly influenced by genetic withdrawal vulnerability. The dimorphic response during abstinence was noted by unsupervised hierarchical cluster analysis, with 100% support for separation based on genotype/withdrawal phenotype in bootstrap analysis (Figure 1a). Expression differences identified in the array hybridizations were confirmed by qRT-PCR (Table 1), and validated *in vivo* by biochemical, physiological and behavioral outcomes. In both male and female WSR mice, expression differences indicated increased apoptosis (Figure 2) that was confirmed in histological analysis of PFC (Figure 3). Further *in vivo* validation of significant pathways demonstrated increased circulating thyroid hormone levels in abstinent WSR mice (Figure 4). Most importantly, behavioral validation of the expression differences was presented, with inhibition of thyroid hormone signaling associated with a reduction in voluntary relapse EtOH drinking in WSR mice (Figure 5).

Divergent response between selected phenotype/genotype during abstinence

In this study we modeled the final stage of the addiction cycle as described by Koob and Volkow (Koob and Volkow, 2010), *i.e.*, intoxication, withdrawal and craving/abstinence, by characterizing neuroadaptive changes in PFC following a prolonged period of abstinence after withdrawal from chronic intoxication. The potential influence of genotype/withdrawal phenotype on neuroadaptive changes present during abstinence was evaluated by employing the WSR and WSP lines, selected from heterogeneous stock for divergent withdrawal severity after chronic intoxication. During the immediate withdrawal period, strong sexual dimorphism had been observed in WSR and WSP mice with respect to changes in neurotoxicity and expression differences (Hashimoto and Wiren, 2008) and in serum testosterone concentrations (Forquer et al., 2010). Contrasting with such results where sex was an important influence on responsiveness observed during withdrawal, genotype/withdrawal phenotype appeared to have more influence on the neuroadaptive response after a sustained period of abstinence. Interestingly, 28 % of all genes regulated during abstinence

were also differentially expressed between naïve WSP and WSR, suggesting that a portion of the genes enriched by selection pressure also represented a neuroadaptive target during abstinence. In addition, a large percentage of genes that were significantly different from controls at peak withdrawal after intoxication were also different during abstinence in the same group, suggesting persistent regulation after chronic intoxication and withdrawal.

Groups of genes that demonstrated the greatest dimorphism between the WSR and WSP lines were identified by *k*-means clustering (Figure 1). Several overrepresented GO categories were of interest in the highly dimorphic response genes, including acetylases/ histone deacetylases involved in chromatin remodeling (Table 3), which suggests a potential epigenetic mechanism for persistently regulated genes during abstinence. A better understanding of expression differences that persist in abstinence is likely of great consequence since it has been proposed that they may play a critical role to influence relapse potential in the recovering alcoholic (Wiren et al., 2006).

Response to EtOH as a model of human alcoholism

Although controversial (Morean and Corbin, 2010), one group of individuals with a greater risk for the development of alcohol use disorders (AUDs) typically have a lower subjective response to the effects of EtOH (Schuckit, 2009). The low response endophenotype, with increased voluntary EtOH consumption and a low level of ataxic response to alcohol, can be a strong predictor of developing alcohol dependency in both males and females (Schuckit et al., 2000). Interestingly, similarities exist between the WSR line and characteristics of this low response alcoholic intermediate phenotype that include increased voluntary EtOH consumption (Kosobud et al., 1988), decreased response during withdrawal from chronic EtOH exposure (Kosobud and Crabbe, 1986), decreased sensitivity to EtOH-induced conditioned place preference (Crabbe et al., 1992) and increased voluntary relapse drinking shown here. Expression differences identified in our analysis may provide insight into treatment options for a specific subset of alcoholic patients as it has been proposed that effective treatments for alcoholism will likely result from targeting of specific phenotypes rather than employing a broad and uniform approach (Kuehn, 2009).

Although there are no reports detailing brain expression differences observed during a defined period of abstinence, analysis has been performed on post-mortem tissue from human alcoholics at various stages of intoxication and withdrawal. These reports have identified several functional groups including immune response and inflammation, cell survival, signal transduction and energy production (see Okvist et al., 2007). Furthermore, multiple genes involved in myelination, protein trafficking and apoptosis were found to be differentially expressed in the brains (especially prefrontal cortex) after chronic alcohol abuse (Flatscher-Bader et al., 2005, Alexander-Kaufman et al., 2006, Liu et al., 2006). As shown in this report, several of the more highly regulated sequences we identified (Table 2) have been implicated in inflammatory signaling including *Lgals1*, *Heximl, Ifi203* and *Hmha1* (Dey et al., 2007, Malik et al., 2009, Nicholls et al., 2009, Mondini et al., 2010) while *Spo11, Rere, Zfp618, Zfp653* and *Mn1* function in the transcription factors /DNA binding/chromatin remodeling group (Sutton et al., 2005, Wang et al., 2008, Kidane et al., 2010) and *Vps13d, Rere* and *Map4k4* are associated with neurodegenerative disorders and/or epileptic electrical activity (Arion et al., 2006, Kurano et al., 2007, Wang and Tsai, 2008). In addition, lipid metabolism and lipid biosynthesis were significant categories in GO analysis for female WSR and male WSP mice respectively. The similar responses identified in humans and in this report may reflect persistent alterations that occur over time in chronic alcoholics.

Hormone dysfunction during abstinence

Thyroid hormone dysfunction in alcoholic populations has been repeatedly described (Hermann et al., 2002). Here we observed a dimorphic response in TTR and T3 levels between WSR and WSP mice, with increased thyroid hormone signaling during abstinence in WSR mice but inhibition of signaling in WSP mice (Figure 4). Thyroid dysfunction in alcoholics during detoxification and abstinence remains controversial, with descriptions of no effect, elevations or inhibition of T3 or T4 levels (Valimaki et al., 1984, Baumgartner et al., 1994, Pienaar et al., 1995, Ozsoy et al., 2006). Based on findings reported here, some of the variation observed in the literature may reflect an underlying genetic contribution to the response during abstinence in humans. Changes in thyroid hormone levels may have important consequences in alcoholics. For example, sustained elevation of thyroid hormone levels or frank thyrotoxicosis can influence sympathetic tone, and novel neural pathways influenced by thyroid hormone have been described (Fliers et al., 2010). Elevations of thyroid hormone levels and the associated increase in sympathetic tone may play a role in cardiac arrhythmia and unexpected death in alcoholics during withdrawal (Liu and Fujimiya, 2010). Interestingly, elevated free T3 level has been directly correlated with a psychological assessment of craving in alcohol dependent patients at 12 weeks of detoxification (Leggio et al., 2008). Consistent with these changes, we also identified ‘response to hormone stimulus’ and ‘thyroid gland development’ as GO categories that were the most dimorphic between WSR and WSP mice during abstinence (Table 3). In addition, serum testosterone levels are elevated during abstinence in both sexes of WSR mice but not in WSP mice (Forquer et al., 2010). Increased testosterone levels are also observed in some alcoholics after detoxification for 21 d (King et al., 1995, Ruusa et al., 1997). Thus, increased thyroid hormone levels and/or increased serum testosterone levels observed in WSR mice during abstinence in both sexes may also be associated with an alcoholic phenotype. Such endocrine dysregulation would likely have an important impact in the abstinent alcoholic.

Active process of neurodegeneration during abstinence

Gene expression differences were identified in PFC, a brain region associated with cognitive dysfunction and damage in alcoholics (Gazdzinski et al., 2005, Harper and Matsumoto, 2005). Genes involved in apoptosis and cell death showed differential regulation between WSR and WSP mice, with increased apoptosis predicted in WSR mice. Confirmation of this result was demonstrated with a significant increase in dead cells in PFC of WSR mice but not WSP mice. The significant increase in dead cells observed in WSR mice raise concern that by extension, low response individuals might also have enhanced PFC damage. Importantly, dead cells are rapidly cleared from the brain and 21d following an excitotoxic insult, dead cells are no longer present (Benkovic et al., 2004). Thus, the apoptotic/cell death signaling and the presence of increase number of dead cells suggest an active process of neurodegeneration during abstinence in WSR mice. Given the importance of PFC function, such damage could underlie debilitating cognitive dysfunction and motor deficits observed in some alcoholics. In addition, disruption of normal PFC inhibitory functions (*i.e.*, inhibition of unnecessary or unwanted behavior) suggest such individuals may be more likely to suffer from relapse after a period of abstinence, to contribute to excessive drinking and the self-sustaining nature of alcoholism.

Conclusion

Alcohol abuse and relapse after abstinence remain serious public health concerns that are ineffectively treated with currently available therapies. In this study, we have identified gene targets that are altered during abstinence in PFC after chronic EtOH intoxication, and determined that these neuroadaptive changes influence relapse drinking. Using an animal model with highly divergent withdrawal response, we employed microarray hybridization and bioinformatic analyses and confirmed the biological relevance of expression changes

identified in abstinence after chronic EtOH intoxication. Results revealed that the transcriptional response during abstinence was strongly influenced by genotype/withdrawal phenotype and not sex. Relapse drinking was reduced in low response mice after intervention in signaling pathways identified, and results suggest increased risk for relapse in low response abstinent populations. As the influence of genetic background on alcohol disorders remains an area of intense debate, these results provide a rationale for targeted treatment approaches in abstinent alcoholics that group in a low response phenotype. Identification of signaling pathways altered in abstinence using animal models may aid development of novel therapeutics for the targeted treatment of relapse of abstinent alcoholics.

Research Highlights

- Transcriptional profiling performed in an animal model of abstinence after alcohol abuse
- Neuroadaptive response during abstinence is determined by phenotype/genetic background
- Relapse drinking was reduced by inhibition of thyroid hormone synthesis

Acknowledgments

The authors gratefully acknowledge the support of Drs. John Crabbe and Pamela Metten for providing the WSR and WSP mice and for assistance with chronic alcohol exposure. This work was made possible by grants from the Department of Veterans Affairs Merit Review program (KMW) and the National Institute of Alcoholism and Alcohol Abuse R01 AA013194 (KMW) and R01 AA012439 (DAF). All work was performed in facilities provided by the Department of Veterans Affairs.

References

Adachi J, Mizoi Y, Fukunaga T, Ogawa Y, Ueno Y, Imamichi H. Degrees of alcohol intoxication in 117 hospitalized cases. J Stud Alcohol. 1991; 52:448–453. [PubMed: 1943100]

Addolorato G, Capristo E, Caputo F, Greco AV, Ceccanti M, Stefanini GF, Gasbarrini G. Nutritional status and body fluid distribution in chronic alcoholics compared with controls. Alcohol Clin Exp Res. 1999; 23:1232–1237. [PubMed: 10443991]

Alexander-Kaufman K, James G, Sheedy D, Harper C, Matsumoto I. Differential protein expression in the prefrontal white matter of human alcoholics: a proteomics study. Mol Psychiatry. 2006; 11:56–65. [PubMed: 16172612]

Arion D, Sabatini M, Unger T, Pastor J, Alonso-Nanclares L, Ballesteros-Yanez I, Garcia Sola R, Munoz A, Mirnics K, DeFelipe J. Correlation of transcriptome profile with electrical activity in temporal lobe epilepsy. Neurobiol Dis. 2006; 22:374–387. [PubMed: 16480884]

Baraona E, Abittan CS, Dohmen K, Moretti M, Pozzato G, Chayes ZW, Schaefer C, Lieber CS. Gender differences in pharmacokinetics of alcohol. Alcohol Clin Exp Res. 2001; 25:502–507. [PubMed: 11329488]

Baumgartner A, Rommelspacher H, Otto M, Schmidt LG, Kurten I, Graf KJ, Campos-Barros A, Platz W. Hypothalamic-pituitary-thyroid (HPT) axis in chronic alcoholism. I. HPT axis in chronic alcoholics during withdrawal and after 3 weeks of abstinence. Alcohol Clin Exp Res. 1994; 18:284–294. [PubMed: 8048729]

Beadles-Bohling AS, Wiren KM. Anticonvulsive effects of kappa-opioid receptor modulation in an animal model of ethanol withdrawal. Genes Brain Behav. 2006; 5:483–496. [PubMed: 16923153]

Becker HC, Lopez MF. Increased ethanol drinking after repeated chronic ethanol exposure and withdrawal experience in C57BL/6 mice. Alcohol Clin Exp Res. 2004; 28:1829–1838. [PubMed: 15608599]

Benkovic SA, O'Callaghan JP, Miller DB. Sensitive indicators of injury reveal hippocampal damage in C57BL/6J mice treated with kainic acid in the absence of tonic-clonic seizures. Brain Res. 2004; 1024:59–76. [PubMed: 15451367]

Bertucci F, Bernard K, Loriod B, Chang YC, Granjeaud S, Birnbaum D, Nguyen C, Peck K, Jordan BR. Sensitivity issues in DNA array-based expression measurements and performance of nylon microarrays for small samples. Hum Mol Genet. 1999; 8:1715–1722. [PubMed: 10441335]

Brady K, Randall C. Gender differences in substance use disorders. Psychiatr Clin North Am. 1999; 22:241–252. [PubMed: 10385931]

Brooks SP, Croft AP, Norman G, Shaw SG, Little HJ. Nimodipine prior to alcohol withdrawal prevents memory deficits during the abstinence phase. Neuroscience. 2008; 157:376–384. [PubMed: 18835336]

Cano-Europa E, Blas-Valdivia V, Lopez-Galindo GE, Franco-Colin M, Pineda-Reynoso M, Hernandez-Garcia A, Ortiz-Butron R. Methimazole-induced hypothyroidism causes alteration of the REDOX environment, oxidative stress, and hepatic damage; events not caused by hypothyroidism itself. Ann Hepatol. 2010; 9:80–88. [PubMed: 20308726]

Carroll M, Lynch W, Roth M, Morgan A, Cosgrove K. Sex and estrogen influence drug abuse. Trends Pharmacol Sci. 2004; 25:273–279. [PubMed: 15120494]

Crabbe JC, Phillips TJ, Cunningham CL, Belknap JK. Genetic determinants of ethanol reinforcement. Ann N Y Acad Sci. 1992; 654:302–310. [PubMed: 1632589]

Dai M, Wang P, Boyd AD, Kostov G, Athey B, Jones EG, Bunney WE, Myers RM, Speed TP, Akil H, Watson SJ, Meng F. Evolving gene/transcript definitions significantly alter the interpretation of GeneChip data. Nucleic Acids Res. 2005; 33:e175. [PubMed: 16284200]

Dennis G Jr. Sherman BT, Hosack DA, Yang J, Gao W, Lane HC, Lempicki RA. DAVID: Database for Annotation, Visualization, and Integrated Discovery. Genome Biol. 2003; 4:P3. [PubMed: 12734009]

Devaud L, Chadda R. Sex differences in rats in the development of and recovery from ethanol dependence assessed by changes in seizure susceptibility. Alcohol Clin Exp Res. 2001; 25:1689–1696. [PubMed: 11707644]

Dey A, Chao SH, Lane DP. HEXIM1 and the control of transcription elongation: from cancer and inflammation to AIDS and cardiac hypertrophy. Cell Cycle. 2007; 6:1856–1863. [PubMed: 17671421]

Flatscher-Bader T, van der Brug M, Hwang J, Gochee P, Matsumoto I, Niwa S, Wilce P. Alcohol-responsive genes in the frontal cortex and nucleus accumbens of human alcoholics. J Neurochem. 2005; 93:359–370. [PubMed: 15816859]

Fliers E, Klieverik LP, Kalsbeek A. Novel neural pathways for metabolic effects of thyroid hormone. Trends Endocrinol Metab. 2010; 21:230–236. [PubMed: 20005733]

Forquer M, Hashimoto J, Roberts M, Wiren K. Elevated testosterone in females reveals a robust sex difference in altered androgen levels during chronic alcohol withdrawal. Alcohol. 2010 in press.

Gazdzinski S, Durazzo TC, Meyerhoff DJ. Temporal dynamics and determinants of whole brain tissue volume changes during recovery from alcohol dependence. Drug Alcohol Depend. 2005; 78:263–273. [PubMed: 15893157]

Goldstein DB, Pal N. Comparison of pyrazole and 4-brompyrazole as inhibitors of alcohol dehydrogenases: their potency, toxicity and duration of action in mice. J Pharmacol Exp Ther. 1971; 178:199–203. [PubMed: 5089709]

Griffin WC 3rd, Lopez MF, Becker HC. Intensity and duration of chronic ethanol exposure is critical for subsequent escalation of voluntary ethanol drinking in mice. Alcohol Clin Exp Res. 2009a; 33:1893–1900. [PubMed: 19673744]

Griffin WC 3rd, Lopez MF, Yanke AB, Middaugh LD, Becker HC. Repeated cycles of chronic intermittent ethanol exposure in mice increases voluntary ethanol drinking and ethanol concentrations in the nucleus accumbens. Psychopharmacology (Berl). 2009b; 201:569–580. [PubMed: 18791704]

Hansson AC, Nixon K, Rimondini R, Damadzic R, Sommer WH, Eskay R, Crews FT, Heilig M. Long-term suppression of forebrain neurogenesis and loss of neuronal progenitor cells following prolonged alcohol dependence in rats. Int J Neuropsychopharmacol. 2010:1–11. PMID: 20334723.

Harper C, Matsumoto I. Ethanol and brain damage. Curr Opin Pharmacol. 2005; 5:73–78. [PubMed: 15661629]

Hashimoto JG, Beadles-Bohling AS, Wiren KM. Comparison of RiboGreen and 18S rRNA quantitation for normalizing real-time RT-PCR expression analysis. Biotechniques. 2004; 36:54–56. 58–60. [PubMed: 14740484]

Hashimoto JG, Wiren KM. Neurotoxic consequences of chronic alcohol withdrawal: expression profiling reveals importance of gender over withdrawal severity. Neuropsychopharmacology. 2008; 33:1084–1096. [PubMed: 17593928]

Hermann D, Heinz A, Mann K. Dysregulation of the hypothalamic-pituitary-thyroid axis in alcoholism. Addiction. 2002; 97:1369–1381. [PubMed: 12410778]

Huang da W, Sherman BT, Lempicki RA. Systematic and integrative analysis of large gene lists using DAVID bioinformatics resources. Nat Protoc. 2009; 4:44–57. [PubMed: 19131956]

Kidane D, Jonason AS, Gorton TS, Mihaylov I, Pan J, Keeney S, de Rooij DG, Ashley T, Keh A, Liu Y, Banerjee U, Zelterman D, Sweasy JB. DNA polymerase beta is critical for mouse meiotic synapsis. Embo J. 2010; 29:410–423. [PubMed: 20019666]

King AC, Errico AL, Parsons OA. Eysenck's personality dimensions and sex steroids in male abstinent alcoholics and nonalcoholics: an exploratory study. Biol Psychol. 1995; 39:103–113. [PubMed: 7734625]

Koob G, Volkow N. Neurocircuitry of addiction. Neuropsychopharmacology. 2010; 35:217–238. [PubMed: 19710631]

Kosobud A, Bodor A, Crabbe J. Voluntary consumption of ethanol in WSP, WSC and WSR selectively bred mouse lines. Pharmacol Biochem Behav. 1988; 29:601–607. [PubMed: 3362955]

Kosobud A, Crabbe J. Ethanol withdrawal in mice bred to be genetically prone or resistant to ethanol withdrawal seizures. J Pharmacol Exp Ther. 1986; 238:170–177. [PubMed: 3723396]

Kuehn BM. Findings on alcohol dependence point to promising avenues for targeted therapies. JAMA. 2009; 301:1643–1645. [PubMed: 19383946]

Kurano Y, Nakamura M, Ichiba M, Matsuda M, Mizuno E, Kato M, Agemura A, Izumo S, Sano A. In vivo distribution and localization of chorein. Biochem Biophys Res Commun. 2007; 353:431–435. [PubMed: 17188237]

Leggio L, Ferrulli A, Cardone S, Malandrino N, Mirijello A, D'Angelo C, Vonghia L, Miceli A, Capristo E, Kenna GA, Gasbarrini G, Swift RM, Addolorato G. Relationship between the hypothalamic-pituitary-thyroid axis and alcohol craving in alcohol-dependent patients: a longitudinal study. Alcohol Clin Exp Res. 2008; 32:2047–2053. [PubMed: 18828809]

Leh SE, Petrides M, Strafella AP. The neural circuitry of executive functions in healthy subjects and Parkinson's disease. Neuropsychopharmacology. 2010; 35:70–85. [PubMed: 19657332]

Liu J, Fujimiya T. Abrupt termination of an ethanol regimen provokes ventricular arrhythmia and enhances susceptibility to the arrhythmogenic effects of epinephrine in rats. Alcohol Clin Exp Res. 2010; 34(Suppl 1):S45–53. [PubMed: 19094192]

Liu J, Lewohl J, Harris R, Iyer V, Dodd P, Randall P, Mayfield R. Patterns of gene expression in the frontal cortex discriminate alcoholic from nonalcoholic Individuals. Neuropsychopharmacology. 2006; 31:1574–1582. [PubMed: 16292326]

Magnusson A, Goransson M, Heilig M. Early onset alcohol dependence with high density of family history is not "male limited". Alcohol. 2010; 44:131–139. [PubMed: 20193873]

Malik RK, Ghurye RR, Lawrence-Watt DJ, Stewart HJ. Galectin-1 stimulates monocyte chemotaxis via the p44/42 MAP kinase pathway and a pertussis toxin-sensitive pathway. Glycobiology. 2009; 19:1402–1407. [PubMed: 19561030]

Matsumoto I. Proteomics approach in the study of the pathophysiology of alcohol-related brain damage. Alcohol Alcohol. 2009; 44:171–176. [PubMed: 19136498]

Melendez RI, Middaugh LD, Kalivas PW. Development of an alcohol deprivation and escalation effect in C57BL/6J mice. Alcohol Clin Exp Res. 2006; 30:2017–2025. [PubMed: 17117967]

Mondini M, Costa S, Sponza S, Gugliesi F, Gariglio M, Landolfo S. The interferon-inducible HIN-200 gene family in apoptosis and inflammation: implication for autoimmunity. Autoimmunity. 2010; 43:226–231. [PubMed: 20187706]

Morean ME, Corbin WR. Subjective response to alcohol: a critical review of the literature. Alcohol Clin Exp Res. 2010; 34:385–395. [PubMed: 20028359]

Morrow AL, Biggio G, Serra M, Becker HC, Lopez MF, Porcu P, Alward SE, O'Buckley TK. The role of neuroactive steroids in ethanol/stress interactions: proceedings of symposium VII at the Volterra conference on alcohol and stress, May 2008. Alcohol. 2009; 43:521–530. [PubMed: 19913195]

Nicholls S, Piper KP, Mohammed F, Dafforn TR, Tenzer S, Salim M, Mahendra P, Craddock C, van Endert P, Schild H, Cobbold M, Engelhard VH, Moss PA, Willcox BE. Secondary anchor polymorphism in the HA-1 minor histocompatibility antigen critically affects MHC stability and TCR recognition. Proc Natl Acad Sci U S A. 2009; 106:3889–3894. [PubMed: 19234124]

Nixon K, Kim DH, Potts EN, He J, Crews FT. Distinct cell proliferation events during abstinence after alcohol dependence: microglia proliferation precedes neurogenesis. Neurobiol Dis. 2008; 31:218–229. [PubMed: 18585922]

Okvist A, Johansson S, Kuzmin A, Bazov I, Merino-Martinez R, Ponomarev I, Mayfield RD, Harris RA, Sheedy D, Garrick T, Harper C, Hurd YL, Terenius L, Ekstrom TJ, Bakalkin G, Yakovleva T. Neuroadaptations in human chronic alcoholics: dysregulation of the NF-kappaB system. PLoS One. 2007; 2:e930. [PubMed: 17895971]

Olive MF. Pharmacotherapies for alcoholism: the old and the new. CNS Neurol Disord Drug Targets. 2010; 9:2–4. [PubMed: 20232494]

Ozsoy S, Esel E, Izgi HB, Sofuoglu S. Thyroid function in early and late alcohol withdrawal: relationship with aggression, family history, and onset age of alcoholism. Alcohol Alcohol. 2006; 41:515–521. [PubMed: 16855000]

Pereira EF, Aracava Y, Aronstam RS, Barreiro EJ, Albuquerque EX. Pyrazole, an alcohol dehydrogenase inhibitor, has dual effects on N-methyl-D-aspartate receptors of hippocampal pyramidal cells: agonist and noncompetitive antagonist. J Pharmacol Exp Ther. 1992; 261:331–340. [PubMed: 1313873]

Pfefferbaum A, Adalsteinsson E, Sullivan EV. Supratentorial profile of white matter microstructural integrity in recovering alcoholic men and women. Biol Psychiatry. 2006; 59:364–372. [PubMed: 16125148]

Pienaar WP, Roberts MC, Emsley RA, Aalbers C, Taljaard FJ. The thyrotropin releasing hormone stimulation test in alcoholism. Alcohol Alcohol. 1995; 30:661–667. [PubMed: 8554651]

Prescott C, Caldwell C, Carey G, Vogler G, Trumbetta S, Gottesman I. The Washington University Twin Study of alcoholism. Am J Med Genet B Neuropsychiatr Genet. 2005; 134:48–55. [PubMed: 15704214]

Richardson SJ. Cell and molecular biology of transthyretin and thyroid hormones. Int Rev Cytol. 2007; 258:137–193. [PubMed: 17338921]

Rodd ZA, Bertsch BA, Strother WN, Le-Niculescu H, Balaraman Y, Hayden E, Jerome RE, Lumeng L, Nurnberger JI Jr. Edenberg HJ, McBride WJ, Niculescu AB. Candidate genes, pathways and mechanisms for alcoholism: an expanded convergent functional genomics approach. Pharmacogenomics J. 2007; 7:222–256. [PubMed: 17033615]

Ruusa J, Bergman B, Sundell ML. Sex hormones during alcohol withdrawal: a longitudinal study of 29 male alcoholics during detoxification. Alcohol Alcohol. 1997; 32:591–597. [PubMed: 9373701]

Saeed AI, Sharov V, White J, Li J, Liang W, Bhagabati N, Braisted J, Klapa M, Currier T, Thiagarajan M, Sturn A, Snuffin M, Rezantsev A, Popov D, Ryltsov A, Kostukovich E, Borisovsky I, Liu Z, Vinsavich A, Trush V, Quackenbush J. TM4: a free, open-source system for microarray data management and analysis. Biotechniques. 2003; 34:374–378. [PubMed: 12613259]

Sanchis-Segura C, Spanagel R. Behavioural assessment of drug reinforcement and addictive features in rodents: an overview. Addict Biol. 2006; 11:2–38. [PubMed: 16759333]

Schafer GL, Crabbe JC, Wiren KM. Identification of neuroendocrine-specific protein as an ethanol-regulated gene with mRNA differential display. Mamm Genome. 1998; 9:979–982. [PubMed: 9880663]

Schuckit MA. Alcohol-use disorders. Lancet. 2009; 373:492–501. [PubMed: 19168210]

Schuckit MA, Smith TL, Kalmijn J, Tsuang J, Hesselbrock V, Bucholz K. Response to alcohol in daughters of alcoholics: a pilot study and a comparison with sons of alcoholics. Alcohol Alcohol. 2000; 35:242–248. [PubMed: 10869242]

Sershen H, Hashim A, Vadasz C. Strain and sex differences in repeated ethanol treatment-induced motor activity in quasi-congenic mice. Genes Brain Behav. 2002; 1:156–165. [PubMed: 12884971]

Sutton AL, Zhang X, Ellison TI, Macdonald PN. The 1,25(OH)2D3-regulated transcription factor MN1 stimulates vitamin D receptor-mediated transcription and inhibits osteoblastic cell proliferation. Mol Endocrinol. 2005; 19:2234–2244. [PubMed: 15890672]

Tang R, Zhu Z, Qu Y, Li J, Ji Y, Cai Q, Liu B, Yan M, Yin H, Lin Y. The impact of hyperthermic chemotherapy on human gastric cancer cell lines: Preliminary results. Oncol Rep. 2006; 16:631–641. [PubMed: 16865266]

Terdal E, Crabbe J. Indexing withdrawal in mice: Matching genotypes for exposure in studies using ethanol vapor inhalation. Alcohol Clin Exp Res. 1994; 18:542–547. [PubMed: 7943652]

Treadwell JA, Pagniello KB, Singh SM. Genetic segregation of brain gene expression identifies retinaldehyde binding protein 1 and syntaxin 12 as potential contributors to ethanol preference in mice. Behav Genet. 2004; 34:425–439. [PubMed: 15082940]

Valdez GR, Koob GF. Allostasis and dysregulation of corticotropin-releasing factor and neuropeptide Y systems: implications for the development of alcoholism. Pharmacol Biochem Behav. 2004; 79:671–689. [PubMed: 15582675]

Valdez GR, Zorrilla EP, Roberts AJ, Koob GF. Antagonism of corticotropin-releasing factor attenuates the enhanced responsiveness to stress observed during protracted ethanol abstinence. Alcohol. 2003; 29:55–60. [PubMed: 12782246]

Valimaki M, Pelkonen R, Harkonen M, Ylikahri R. Hormonal changes in noncirrhotic male alcoholics during ethanol withdrawal. Alcohol Alcohol. 1984; 19:235–242. [PubMed: 6508878]

Wang G, Volkow N, Fowler J, Franceschi D, Wong C, Pappas N, Netusil N, Zhu W, Felder C, Ma Y. Alcohol intoxication induces greater reductions in brain metabolism in male than in female subjects. Alcohol Clin Exp Res. 2003a; 27:909–917. [PubMed: 12824811]

Wang J, Williams RW, Manly KF. WebQTL: web-based complex trait analysis. Neuroinformatics. 2003b; 1:299–308. [PubMed: 15043217]

Wang L, Charroux B, Kerridge S, Tsai CC. Atrophin recruits HDAC1/2 and G9a to modify histone H3K9 and to determine cell fates. EMBO Rep. 2008; 9:555–562. [PubMed: 18451879]

Wang L, Tsai CC. Atrophin proteins: an overview of a new class of nuclear receptor corepressors. Nucl Recept Signal. 2008; 6:e009. [PubMed: 19043594]

Wetterling T, Veltrup C, Driessen M, John U. Drinking pattern and alcohol-related medical disorders. Alcohol Alcohol. 1999; 34:330–336. [PubMed: 10414607]

Williams TM, Davies SJ, Taylor LG, Daglish MR, Hammers A, Brooks DJ, Nutt DJ, Lingford-Hughes A. Brain opioid receptor binding in early abstinence from alcohol dependence and relationship to craving: an [11C]diprenorphine PET study. Eur Neuropsychopharmacol. 2009; 19:740–748. [PubMed: 19595579]

Wiren KM, Hashimoto JG, Alele PE, Devaud LL, Price KL, Middaugh LD, Grant KA, Finn DA. Impact of sex: determination of alcohol neuroadaptation and reinforcement. Alcohol Clin Exp Res. 2006; 30:233–242. [PubMed: 16441272]

Yoneyama N, Crabbe JC, Ford MM, Murillo A, Finn DA. Voluntary ethanol consumption in 22 inbred mouse strains. Alcohol. 2008; 42:149–160. [PubMed: 18358676]

Zhang B, Schmoyer D, Kirov S, Snoddy J. GOTree Machine (GOTM): a web-based platform for interpreting sets of interesting genes using Gene Ontology hierarchies. BMC Bioinformatics. 2004; 5:16. [PubMed: 14975175]

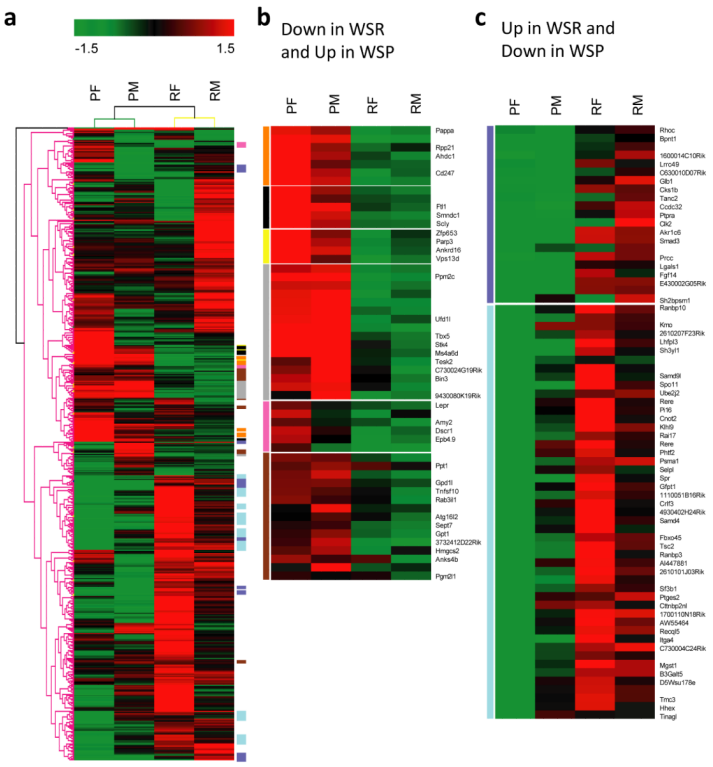

Figure 1.

Hierarchical and *k*-means cluster analysis of genes significantly regulated by chronic EtOH exposure following a period of abstinence. (a). Hierarchical cluster analysis of EtOH regulated genes shows female WSP and male WSP have a more similar expression pattern compared to WSR male and females, which is supported by Boot-strap analysis (Black nodes have 100% support). Individual genes that clustered into the highly dimorphic clusters using *k*-means clustering are identified by a color-coded band to the right of each gene (b&c). *K*-means clustering identified 32 clusters, with ~30% highly dimorphic between WSR and WSP male and female mice. (b). Genes that were down-regulated in WSR but up-regulated in WSP. (c). Genes that were up-regulated in WSR but down-regulated in WSP.

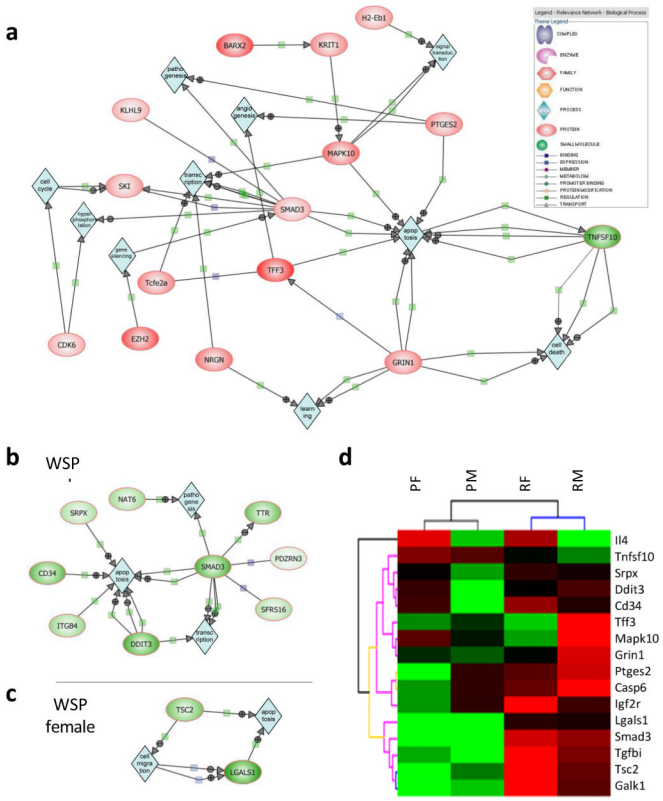

Figure 2.

Pathway Architect ‘Biological Process’ analysis of expression patterns identifies ‘Apoptosis’ as an important target following chronic intoxication and abstinence. In general, apoptosis related genes are up-regulated by EtOH in WSR and down-regulated by EtOH in WSP. (a). Male WSR ‘Biological Process’ relevance network identified Apoptosis related genes Tff3, Smad3, Mapk10, Ptges2, Grin1, and Tnfsf10, which were significantly regulated in male WSR mice at 21 d following chronic EtOH exposure. Other targeted nodes include ‘signal transduction’, ‘cell death’, and ‘learning’. (b). Male WSP ‘Biological Process’ analysis identified apoptosis related genes Smad3, Ddit3, Itgb4, Cd34, and Srpx. (c). Female WSP ‘Biological Process’ analysis identified apoptosis related genes Tsc2 and Lgals1. (d). Hierarchical cluster analysis of apoptosis related genes identified by Pathway Architect ‘Biological Process’ relevance network shows differences in apoptosis related gene expression changes between selected lines. Boot-strap analysis supports the separation of expression patterns between selected lines (not sex) with WSR mice showing increased apoptosis related gene expression changes and WSP mice showing decreased apoptosis related gene expression changes.

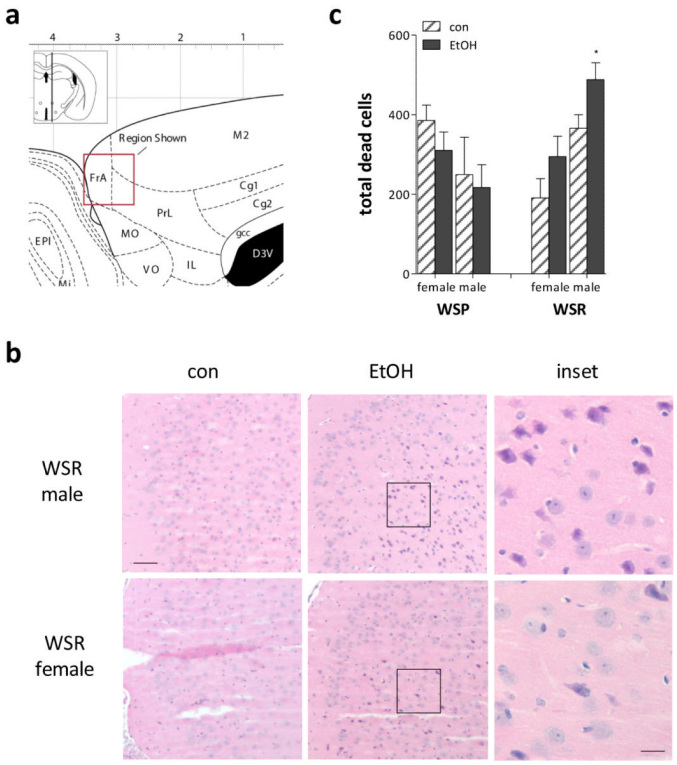

Figure 3.

Histological analysis shows increased cell death in WSR mice after abstinence. (a). Mouse Atlas image of PFC region analyzed for dead cells at 21 d after chronic EtOH intoxication and withdrawal and located approximately anterior 3 mm, ventral 1 mm, and lateral 0.48 mm from Bregma. (abbreviations: FrA – frontal association cortex; M2 – secondary motor cortex; PrL – prelimbic cortex; MO – medial orbital cortex; VO – ventral orbital cortex; IL – infralimbic cortex; D3V – dorsal 3rd ventricle; gcc – genu of corpus callosum; Cg2 – cingulate cortex, area 2; Cg1 – cingulate cortex, area 1; EPl – external plexiform layer of olfactory bulb; Mi – mitral cell layer of olfactory bulb). (b). Quantification of total dead cells in the PFC shows increased cell death in male WSR mice but no differences in WSP mice (n = 9-10). Data are shown as mean ± SEM. *, $p < 0.05$. (c). Representative images of H&E stained brain slices (10x objective) of male and female WSR control (con) mice or mice exposed to chronic EtOH (EtOH). Inset shows a high magnification image from the EtOH condition showing dying cells as hypereosinophilic with pyknotic nuclei (40x objective). Scale bars are 100 μm for the 10x objective images and 25 μm for the 40x objective images.

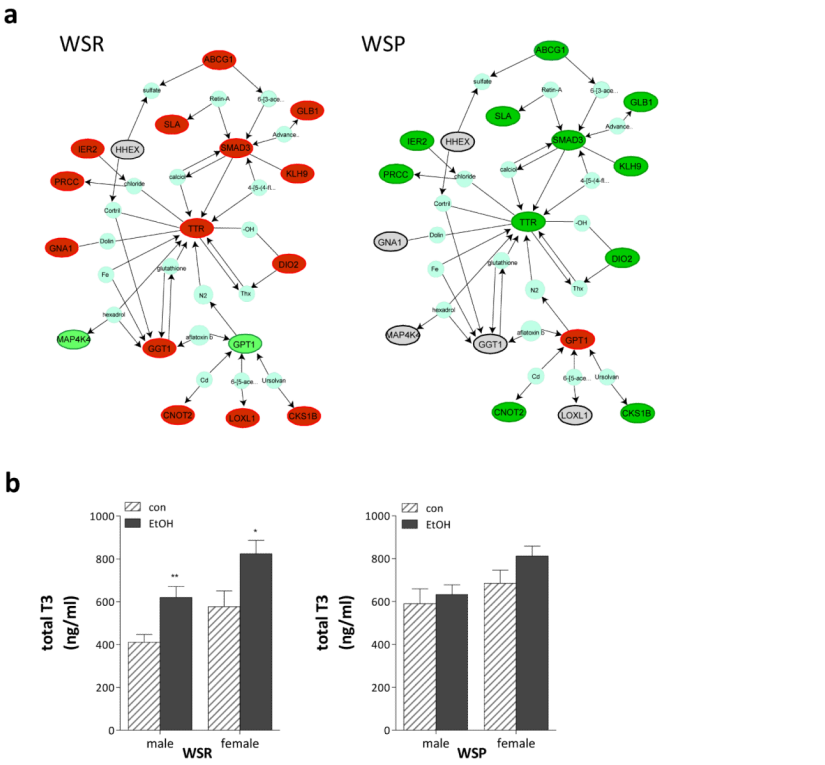

Figure 4.

Physiological confirmation of increased thyroid hormone function in male and female WSR mice during abstinence from chronic EtOH. (a). Pathway Architect 'Small Molecule' network analysis of expression patterns identifies 'TTR' as an important target following chronic intoxication and abstinence. For each gene in the network, red represents up-regulation by EtOH during abstinence in both males and females of each line, green represents down-regulation by EtOH during abstinence in both males and females of each line and grey represents opposite regulation between males and females. In general, thyroid signaling related genes are up-regulated by EtOH in WSR and down-regulated by EtOH in WSP. (b). Confirmation of increased thyroid hormone signaling is shown during abstinence in WSR males and females, with serum total T3 levels significantly increased in both male and female WSR at 21 d after exposure to chronic EtOH with intoxication. No effect was seen in WSP (n = 8-10).

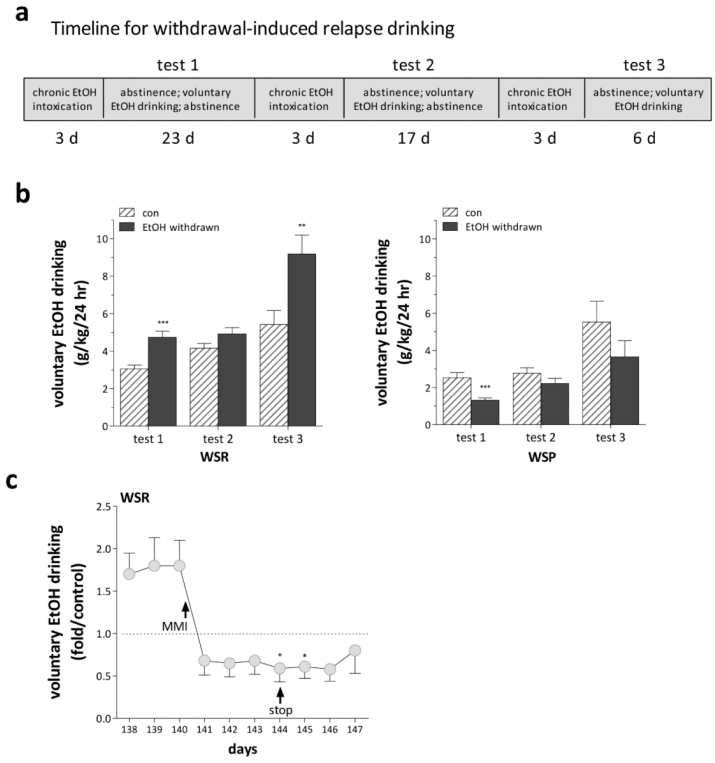

Figure 5.

Behavioral validation for role of altered thyroid hormone signaling in relapse drinking. (a). Timeline for development of relapse drinking model. (b). Chronic intoxication and withdrawal affected withdrawal-induced drinking differently in male WSR and WSP mice. After three episodes of chronic intoxication and brief periods of abstinence, voluntary EtOH drinking was significantly increased in WSR-1 male mice, with no significant effect in WSP-1 mice. Values represent the mean ± SEM for WSR [n = 7-8 for controls and n = 7 (Test 1 & 2) or 5 (Test 3) for EtOH exposed] and WSP [n = 8-9 for controls and n = 7 (Test 1 & 2) or 3 (Test 3) for EtOH exposed] mice. Data are the average intake for 10 d (Test 1) [although intake measured for 18 d, it was only divergent during the 1st 10 d], 11 d (Test 2), or 3 d (Test 3) as these 3 days are the baseline measures prior to injection of MMI. (c). Inhibition of thyroid hormone synthesis in WSR mice by MMI (60 mg/kg/d) in relapse drinking model. Treatment was initiated late on d 3 and was stopped after 5 d. Voluntary EtOH drinking was measured daily for 10 d. Depicted is the change in EtOH intake in the EtOH exposed vs. the control group plotted versus the day of experimentation. MMI reduced voluntary EtOH consumption and inhibited relapse drinking in previously intoxicated WSR mice but not in control WSR mice. Data are shown as mean ± SEM. *, $p < 0.05$; **, $p < 0.01$.

Table 1

Confirmation of genes identified as significantly regulated during abstinence in microarray analysis by qRT-PCR. Ratio data for array data and real-time data are presented as $\log_2$ ratio with *p*-values presented from t-test

		Array Data				Real-Time Data			
Gene	**Comparison**	**Ratio**	**SEM**	**n**	***p*-value**	**Ratio**	**SEM**	**n**	***p*-value**
CD34	Male WSP	−0.61	0.13	4	0.05	0.25	0.18	8	0.47
Ddit3	Male WSP	−0.71	0.11	4	0.02	−0.21	0.13	6	0.44
Dio2	Female WSR	0.77	0.18	4	0.05	0.12	0.11	7	0.56
Dio2	Male WSP	−0.49	0.04	4	0.00	−0.26	0.13	6	0.39
Fbxo45	Female WSP	−0.74	0.14	4	0.01	−0.01	0.16	8	0.69
Fbxo45	Female WSR	0.36	0.08	4	0.03	0.43	0.24	7	0.22
Galk1	Male WSP	−0.38	0.11	4	0.05	−0.24	0.10	7	0.27
Ggt1	Female WSR	0.86	0.19	4	0.03	0.07	0.08	8	0.63
Ggt1	Male WSR	0.41	0.11	4	0.05	0.17	0.07	7	0.40
Grin1	Male WSR	0.42	0.10	4	0.05	−0.03	0.07	8	0.83
Gstp1	Male WSR	0.40	0.18	4	0.05	0.56	0.40	6	0.27
Hexim1	Female WSP	1.21	0.08	4	0.00	0.33	0.36	7	0.54
Hexim1	Female WSR	−0.40	0.05	4	0.02	−0.23	0.05	5	0.25
Ier2	Male WSP	−0.37	0.09	4	0.04	−0.63	0.21	6	0.46
Ier2	Male WSR	0.37	0.09	4	0.05	0.22	0.20	8	0.53
Lgals1	Female WSP	−1.19	0.25	4	0.05	0.60	0.12	8	0.01
Mapk10	Male WSR	0.50	0.17	4	0.04	0.48	0.31	7	0.32
Mgst1	Male WSR	0.34	0.10	4	0.05	0.20	0.11	7	0.38
Parp3	Female WSP	1.01	0.15	4	0.03	0.13	0.08	7	0.29
Parp3	Male WSP	0.34	0.06	4	0.05	0.41	0.15	5	0.07
Ppm2c	Male WSP	0.63	0.07	4	0.01	0.20	0.09	7	0.53
Ppm2c	Male WSR	−0.26	0.04	4	0.03	−0.12	0.08	6	0.61
Smad3	Male WSP	−0.69	0.12	4	0.04	0.01	0.09	8	0.67
Smad3	Male WSR	0.28	0.06	4	0.05	0.24	0.13	8	0.40
Smndc1	Female WSP	1.00	0.15	4	0.03	0.20	0.12	6	0.48
Smndc1	Male WSP	0.40	0.07	4	0.05	0.34	0.07	7	0.02
Stk4	Female WSP	0.69	0.10	4	0.02	0.37	0.09	6	0.14

		Array Data				Real-Time Data			
Gene	Comparison	Ratio	SEM	n	*p*-value	Ratio	SEM	n	*p*-value
Stk4	Male WSP	0.55	0.04	4	0.00	0.39	0.11	7	0.07
Tnfsf10	Male WSR	−0.25	0.08	4	0.03	−0.20	0.06	8	0.34
Tsc2	Female WSP	−0.73	0.20	4	0.05	−0.06	0.05	7	0.59
Ttr	Male WSP	−0.56	0.13	4	0.05	−2.26	0.08	8	0.38
Ttr	Female WSR	0.33	0.06	4	0.05	1.98	1.59	7	0.45

Table 2

The most highly up- or down-regulated named sequences were identified from the list of 562 significantly regulated transcripts. Transcripts are listed in ascending order for each group. Regulation represents log2 fold-change of EtOH vs. control with negative values indicating down-regulation by EtOH and positive values indicating up-regulation by EtOH

Accession	Unigene	Name	Symbol	Ratio
Female WSP				
AI447735	Mm.218624	Sh3 domain YSC-like 1	Sh3yl1	−1.33
AI465143	Mm.43831	Lectin, galactose binding, soluble 1	Lgals1	−1.19
AI662498	Mm.196013	Sterile alpha motif domain containing 9-like	Samd9l	−1.15
AI449549	Mm.23495	Sporulation protein, meiosis-specific, SPO11 homolog (S. cerevisiae)	Spo11	−1.14
AI450210	Mm.291274	Arginine glutamic acid dipeptide (RE) repeats	Rere	−1.09
AI448530	Mm.347707	Zinc finger protein 653	Zfp653	1.13
AI326448	Mm.250256	Ectonucleotide pyrophosphatase/phosphodiesterase 2	Enpp2	1.13
AI413779	Mm.41637	ADP-ribosylation factor interacting protein 2	Arfip2	1.18
AI426204	Mm.478282	Hexamethylene bis-acetamide inducible 1	Hexim1	1.21
AI414560	Mm.4498	Protein tyrosine phosphatase, non-receptor type 14	Ptpn14	1.36
Female WSR				
AI427478	Mm.28146	Mevalonate (diphospho) decarboxylase	Mvd	−0.59
AI464551	Mm.26479	Zinc fingerprotein 618	Zfp618	−0.48
AI452339	Mm.476856	Vacuolar protein sorting 13 D (yeast)	Vps13d	−0.46
AI465256	Mm.19073	Mitogen-activated protein kinase kinase kinase kinase 4	Map4k4	−0.43
AI426204	Mm.478282	Hexamethylene bis-acetamide inducible 1	Hexim1	−0.40
AI452009	Mm.332576	Meningioma 1	Mn1	1.06
AI450557	Mm.334726	G protein-coupled receptor 114	Gpr114	1.10
AI449360	Mm.472787	Interferon activated gene 203	Ifi203	1.16
AI450547	Mm.458468	Kinesin family member 14	Kif14	1.17
AI451660	Mm.222206	Aspartate-beta-hydroxylase	Asph	1.18
Male WSP				
AI414484	Mm.11535	DDB1 and CUL4 associated factor 11	Dcaf11	−0.96
AI414514	Mm.11068	Transmembrane channel-like gene family 5	Tmc5	−0.92
AI430932	Mm.243954	Histocompatibility (minor) HA-1	Hmha1	−0.90
AI428126	Mm.264016	Atlastin GTPase 3	Atl3	−0.89
AI327009	Mm.238817	Ribosomal protein L38	Rpl38	−0.89
AI661257	Mm.261270	Interferon activated gene 203	Ifi203	0.66
AI449169	Mm.209147	Antagonist of mitotic exit network 1 homolog (S. cerevisiae)	Amn1	0.69
AI464523	Mm.103636	T-box 5	Tbx5	0.74
AI464318	Mm.24186	Bridging integrator 3	Bin3	0.84
AI464326	Mm.425201	Testis-specific kinase 2	Tesk2	0.87
Male WSR				

Accession	Unigene	Name	Symbol	Ratio
AI325237	Mm.439727	Amylase 1, salivary	Amy1	−0.36
AI449169	Mm.209147	Antagonist of mitotic exit network 1 homolog (S. cerevisiae)	Amn1	−0.31
AI452087	Mm.23165	Ankyrin repeat and sterile alpha motif domain containing 4B	Anks4b	−0.29
AI429661	Mm.281969	RAB3A interacting protein (rabin3)-like 1	Rab3il1	−0.27
AI426501	Mm.22109	Coiled-coil domain containing 47	Ccdc47	−0.26
AI596353	Mm.274734	NFKB inhibitor interacting Ras-like protein 2	Nkiras2	0.79
AI573426	Mm.389894	Harvey rat sarcoma oncogene, subgroup R	Rras	0.80
AI385732	Mm.30155	ATPase, H+ transporting, lysosomal V0 subunit C	Atp6v0c	0.80
AI426165	Mm.204876	RIKEN cDNA 4931428F04 gene	4931428F04Rik	0.82
AI413436	Mm.297761	CDNA sequence BC006965	BC006965	0.85

Table 3

Overrepresented GO categories identified by DAVID analysis for the group of significantly regulated transcripts that are the most dimorphic between WSR and WSP mice identified using *k*-means clustering from Figure 1

Category	Count	P Value	Symbols
WSR Down-Regulated			
response to hormone stimulus	3	0.018	Rcan1, Lepr, Hmgcs2
response to endogenous stimulus	3	0.022	Rcan1, Lepr, Hmgcs2
regulation of cellular component size	3	0.0376	Epb4.9, Bin3, Ppt1
regulation of hydrolase activity	3	0.0505	Rcan1, Lepr, Ppt1
response to estrogen stimulus	2	0.0534	Rcan1, Lepr
AT hook, DNA-binding, conserved site	2	0.0692	Ahdc1, Zfp653
AT_hook	2	0.0713	Ahdc1, Zfp653
response to steroid hormone stimulus	2	0.0827	Rcan1, Lepr
extracellular space	3	0.0832	Tnfsf10, Lepr, Ppt1
WSR Up-Regulated			
nadp	5	0.0138	Akr1c6, Kmo, Nudt12, Cbr1, Spr
acetylation	13	0.019	Lasp1, Psma1, Lgals1, Cmbl, Cbr1, Spr, Mgst1, Pfn2, Hspe1, Bpnt1, Kctd5, Rbbp4, Rpl38
nucleotide phosphate-binding region:NADP	3	0.0513	Akr1c6, Cbr1, Spr
metal ion transport	6	0.0549	Tsc2, Kctd5, Kctd6, Sri, Grin1, Slc20a2
SPRY	3	0.0588	Fbxo45, Trim68, Ranbp10
histone deacetylase complex	3	0.0629	Rere, Rbbp4, Cbx5
Hyaluronidase	2	0.0637	Nat6
Glycoside hydrolase, family 56	2	0.0637	Nat6
SPla/RYanodine receptor subgroup	3	0.0641	Fbxo45, Trim68, Ranbp10
hyaluronon glucosaminidase activity	2	0.0647	Nat6
B30.2/SPRY	3	0.0696	Fbxo45, Trim68, Ranbp10
heart development	5	0.0829	Zmiz1, Tsc2, Smad3, Hhex
oxidation reduction	8	0.0835	Akr1c6, Kmo, Cyp2c67, Dio2, Gfer, Ndufb7, Cbr1, Spr
thyroid gland development	2	0.0932	Smad3, Hhex
ion transport	7	0.0946	Lasp1, Tsc2, Kctd5, Kctd6, Sri, Grin1, Slc20a2
hexosaminidase activity	2	0.0955	Nat6
Arachidonic acid metabolism	3	0.0969	Cyp2c67, Ptges2, Cbr1
cation transport	6	0.0979	Tsc2, Kctd5, Kctd6, Sri, Grin1, Slc20a2
liver	2	0.0986	Akr1c6, Ttr
cross-link:Glycyl lysine isopeptide (Lys-Gly) (interchain with G-Cter in ubiquitin)	4	0.0992	AW555464, Psma1, Rbbp4, Rps6ka2

Table 4

Overrepresented GO categories identified by DAVID analysis for each group of significantly regulated transcripts

Category	P Value	Symbol
Female WSP		
cellular component unknown	0.0010	Drg2 Cnot2 Sgk2 Sh3yl1 Asb1 Lgals1 Tinagl1
heart development	0.0028	Tbx5 Hhex Hexim1 Gna11
protein amino acid ADP-ribosylation	0.0041	Gna11 Parp3
cellular metabolism	0.0071	46 Genes
electron carrier activity	0.0095	Kmo Dgke
nucleus	0.0100	29 Genes
mRNA processing	0.0113	Smndc1 Sf3b1
protein amino acid ADP-ribosylation	0.0150	Parp3, Gna11
metabolism	0.0160	47 Genes
spliceosome complex	0.0161	Smndc1 Sf3b1
phospholipid biosynthesis	0.0180	Dgke D5Wsu178e
visual perception	0.0250	Gprc5c, Ppt1
sex differentiation	0.0280	Spo11 Asb1
transaminase activity	0.0310	Scly Gfpt1
nucleo base, nucleo side, nucleo tide and nucleic acid metabolism	0.0400	24 Genes
transcription factor activity	0.0420	Tbx5 Rere Tanc2 Tshz2 Hhex Asb1 Tfdp2
biopolymer metabolism	0.0430	21 Genes
Male WSP		
thyroid hormone metabolism	0.0016	Ttr Dio2
extrinsic to plasma membrane	0.0082	Gna11 Rab13
protein amino acid ADP-ribosylation	0.0096	Gna11 Parp3
cell cortex	0.0130	Lasp1 Exoc2
steroid biosynthesis	0.0156	Ugcg Cept1
lipid biosynthesis	0.0160	Ugcg Cept1 Akr1c6 Hmgcs2 Nudt12
RNA splicing	0.0217	Smndc1 Sf3b1 Sfrs16
response to unfolded protein	0.0270	Upf3b Ddit3 Hspe1
transcription factor binding	0.0310	Sub1 Smad3 Ldb1
spliceosome complex	0.0314	Smndc1 Sf3b1
mRNA processing	0.0356	Smndc1 Sf3b1 Sfrs16
protein amino acid ADP-ribosylation	0.0370	Gna11 Parp3
RNA processing	0.0405	Smndc1 Sf3b1 Sfrs16
mRNA metabolism	0.0411	Smndc1 Sf3b1 Sfrs16
oxidoreductase activity, acting on CH-OH group of donors	0.0460	Akr1c6 Cbr1
regulation of immune system process	0.0480	Cfd Smad3
Female WSR		
COPI coated vessicle membrane	0.0001	Copa Copz1 Copz2

Category	P Value	Symbol
Golgi-associated vessicle	0.0005	Copa Copz1 Copz2
membrane-bound vessicle	0.0006	Copz1 Copa Copz2 Dct Cubn
cytoplasmic vessicle	0.0007	Copz1 Copa Copz2 Dct Cubn
COPI-coated vesicle	0.0009	Copz1 Copz2
vessicle	0.0010	Copz1 Copa Copz2 Dct Cubn
thyroid hormone metabolism	0.0011	Dio2 Ttr
vessicle coat	0.0012	Copz1 Copa Copz2
coated vessicle	0.0013	Copa Copz1 Copz2
translation repressor activity	0.0026	Ireb2 Samd4
transporter activity	0.0029	Copa Copz1 Tmc6 Abcg1 Ifi203 Slc35b3 Gfpt1 Ttr Kctd5 Tm9sf2 Cpne3
vessicle membrane	0.0059	Copa Copz1 Copz2
isomerase activity	0.0188	Dct Spo11
DNA recombination	0.0205	Spo11 Xrcc3
amino acid and derivative metabolism	0.0220	Dio2 Gfpt1 Dct Ttr Cubn
mRNA binding	0.0220	Upf3b Ireb2
DNA damage response, signal transduction	0.0270	Ifi203 Atr
Golgi apparatus part	0.0270	Copa Copz1 Copz2
inositol or phosphatidylinositol kinase activity	0.0340	Atr Pip5k1c
microsome	0.0460	Copa Dct H6pd
metalloendopeptidase activity	0.0474	Nln Adamts4
tissue remodeling	0.0480	Ifi203 Itga4 Mn1
heart development	0.0480	Itga4 Hhex Hexmin1
Male WSR		
glutathione transferase activity	0.0002	Ggt1 BC021614 Mgst1
glutathione metabolism	0.0003	Ggt1 BC021614 Mgst1
extracellular region part	0.0005	29 Genes
sodium channel activity	0.0028	Scn1b Accn3
protein binding	0.0043	Hes6 Vil1 Sept7 Dynlrb2 Epb4.9 Senp3 Nrgn Pilra Scrib Kctd5 Tcf3 Pfn2 Klhl9 Stab1 Arid1a Kctd6 Cbx5 Spna2 Krit1 Dusp19 Irf2bp1 Sh2b1 Dstn Smad3 Mfn1 Zbtb17 Lepr Ezh2
extracellular space	0.0043	28 Genes
hydrolase activity, acting on glycosyl bonds	0.0046	Glb1 Amy1
actin filament depolymerization	0.0079	Epb4.9 Spna2 Dstn
viral assembly, maturation, egress, and release	0.0090	Arhgap28 BC040756
lipid transporter activity	0.0100	Lpl Vldlr Hdlbp
catalytic activity	0.0120	76 Genes
vacuolar membrane	0.0140	Vac14 Atp6v0c
protein depolymerization	0.0150	Spna2 Epb4.9 Dstn

Category	P Value	Symbol
axon guidance	0.0152	Efnb3 Ephb1 Cdh4
axonogenesis	0.0201	Efnb3 Ephb1 Cdh4
monovalent inorganic cation transport	0.0220	Svop Scn1b Grin1 Kctd6 Atp6v0c Accn3 Kctd5
sodium ion binding	0.0220	Svop Scn1b Accn3
aromatic compound metabolism	0.0222	Abhd4 Qdpr Abhd5
hydrolase activity	0.0230	35 Genes
intrinsic to plasma membrane	0.0230	Lepr Hnrpm Stab1 Cdc24 Ggt1 Ephb1 Grin1 Kctd6 Gpr56 Kctd5 Accn3
exopeptidase activity	0.0233	Abhd4 Cpn1 Abhd5
cell organization and biogenesis	0.0244	Vil1 Dynlrb2 Epb4.9 Kif3c Pfn2 Arid1a Cbx5 Sh2b1 Rps6ka2 Mfn1 Ezh2
glutathione transferase activity	0.0258	BC021614 Mgst1
lipid metabolism	0.0260	Acoxl Pnpla6 Ptges2 Akr1c6 Lpl Glt25d1 Osbpl7 Vldlr Abhd4 Abhd5 Hdlbp
Ras guanyl-nucleotide exchange factor activity	0.0290	Dnmbp Rab3il1 Plekhg2
peptidase activity	0.0310	Senp3 Usp34 Psma1 Qpctl Cpn1 Abhd4 Abdh5
aminopeptidase activity	0.0373	Abhd4 Abhd5
microtube motor activity	0.0380	Kif20a Kif3c Dnahc6 Dynlrb2
JNK cascade	0.0401	Mapk10 Dusp19
cation channel activity	0.0410	Scn1b Grin1 Kctd6 Kctd5 Accn3
nucleotidyltransferase activity	0.0430	Mybbp1a Polr2g Poln
motor activity	0.0450	Kif20a Kif3c Grin1 Dnahc6 Dynlrb2
dynein complex	0.0450	Dnahc6 Dynlrb2
exopeptidase activity	0.0470	Cpn1 Abhd4 Abhd5
sodium ion transport	0.0480	Svop Scn1b Accn3